Controlling light with light in blue-light plant photoreceptor phototropin

Sukhdev Roy* and Kapil Kulshrestha

Department of Physics and Computer Science,
Dayalbagh Educational Institute, (Deemed University), Dayalbagh,
Agra 282 005, India

We have theoretically analysed all-optical light modulation in the recently discovered LOV2 domain of the blue-light plant photoreceptor phototropin from *Avena sativa* (oat), based on nonlinear intensity-induced excited-state absorption. Transmission of a cw probe laser beam at 660 nm through LOV2 can be controlled by a cw or pulsed pump laser beam at 442 nm. This modulation is sensitive to the small-signal absorption coefficient, rate constants of L-state and absorption cross-section of the ground state. It is shown that in wild-type LOV2 and its mutant LOV2-C39A, the probe beam can be completely switched by the pump laser beam of intensity 50 and 1 kW/cm^2 respectively. The switching response in LOV2 is faster (~μs) than in other photosensitive retinal proteins. We show the applicability of the characteristics in the design of an optically-addressed spatial light modulator and an all-optical switch.

Keywords: All-optical switching, nano-bio-photonics, nonlinear optics, optical computing, phototropin.

CONTROLLING light with light is of tremendous importance for both fundamental and applied science. The key to achieving this capability is a nonlinear optical material. Technological advancements in fabricating nanostructures and manipulating atoms and molecules has revolutionized the applicability of nonlinear optical principles for a wide variety of photonic applications, including, optical bistability, modulation, storage, switching, transmission, frequency conversion, amplification, imaging and even generation of slow light[1–4].

Naturally occurring photosensitive biological molecules optimized over centuries of evolution that exhibit an efficient nonlinear optical response, provide exciting possibilities for photonic applications. Porphyrins and rhodopsin proteins, especially bacteriorhodopsin (bR) protein found in the purple membrane of *Halobacterium halobium*, have by far been the most extensively studied biomolecules for a wide range of applications[5–15].

A switch is the basic building block of information processing systems. There is tremendous research effort focused on investigating novel materials for all-optical information processing to meet the anticipated demand for high-speed high-bandwidth communication and computing. We have recently reported novel designs of low-power all-optical switches, spatial light modulators (SLM) and logic gates with bR and the photoreceptor sensory rhodopsin II (sR II) or phoborhodopsin protein, synthesized from *Natranobacterium pharaonis*, a halophilic, alkaliphilic bacterium also known as *pharaonis* phoborhodopsin (*p*pR), which has received much attention due to its stability and its recent structure elucidation[12–18]. We have also analysed all-optical light modulation in proteorhodopsin (pR), a new family of retinal proteins that has been discovered recently in marine bacterioplankton, and is globally distributed[19–24]. The protein pigments comprising this rhodopsin family seem to be spectrally tuned to different habitats – absorbing light at different wavelengths in accordance with light available in the environment. Since its discovery, ~800 relatives have been identified in samples throughout the world's oceans[19–24].

Rhodopsin proteins undergo conformational changes in a photocycle lasting a few milliseconds[7–12]. Although the earlier intermediates are formed in subpicosecond or picosecond time, overlapping of the absorption spectra of the various intermediates in the visible region, reduces the switching contrast. To realize fast switching, there is a need to explore the possibility of designing new rhodopsin mutants with the required properties or identify other photoreceptors possessing the desired features.

Phototropin, the plant blue-light photoreceptor, has been recently discovered, which is involved in phototropic plant movement, chloroplast relocation and stomatal opening in guard cells[25–27]. Phototropins are a family of membrane-associated flavoproteins. Detailed photochemical and mutational analysis and structural elucidation of phototropin has recently been undertaken[25–40].

There are at least two kinds of phototropin photoreceptors, namely Phot1 and Phot2 that contain two flavin mononucleotide (FMN)-binding LOV (light-, oxygen-, voltage-sensitive) domains at the N-terminus, each consisting of approximately 100 amino acids, and differences in their sequences define them as either LOV1 or LOV2. These photoreceptors have been identified in several species, including *Arabidopsis thaliana*, *Avena sativa* (oat), *Oryza sativa* (rice), *Zea mays* (corn) and *Chlamydomonas reinhardtii*[26–39].

The crystal structure of the LOV2 domain from the fern *Adiantum capillus-veneris* phy3 has been solved recently to 2.7 Å resolution. Phy3 is a chimeric photoreceptor with homology to phytochrome at its N-terminal end and an almost complete phototropin at its C-terminal end. Its LOV2 domain shares 70% sequence homology with the oat phot1 LOV2. The structure indicates that the FMN molecule is held non-covalently within a chromophore-binding pocket. It places the sulphur of cysteine 39 at ~4.2 Å from the C(4a) carbon of the FMN chromophore. These observations are consistent with the light-induced formation of an FMN-cysteinyl adduct[35].

Extraction of oat LOV domains involves cloning of DNA fragments encoding LOV1 and LOV2 domain from

*For correspondence. (e-mail: sukhdevr@hotmail.com)

the cDNA of *A. sativa* nph1 into the bacterial expression vectors pCAL-n and pCAL-n-EK, as a fusion to the calmodulin binding peptide (CBP). The fusion proteins are then expressed in *Escherichia coli* and purified by calmodulin affinity chromatography. Purified samples are washed into clean buffer (5 mM Tris, 5 mM NaCl, pH 8) using centrifugal concentrators and are centrifuged and/or filtered through a 0.2 μm filter prior to use[36,37].

Both LOV1 and LOV2 domains undergo a fully reversible photocycle characterized by photoinduced blue shifts of their major bands, which involves the formation of a flavin-cysteinyl adduct in the LOV domains. The photosensitivities of LOV1 and LOV2 depend on their amino-terminal domains. They are separated by an intervening sequence of variable length. Upon light illumination, the serine/thionine kinase is activated and multiple auto-phosphorylation is observed[35]. Recently, the LOV2 domain from the phy3 receptor of *Adiantum* has also been shown to be a reversible photochromic switch[38].

Recently, the isolated LOV2 domain from *A. sativa* (oat) Phot1 expressed in *E. coli* has been shown to undergo a simple three-state photocycle as shown in Figure 1. It exhibits a large spectral shift of ~113 nm, no overlapping between the absorption spectra of its L-intermediate state (light-activated), initial D-state (dark state) and adduct S-state (signalling state) over a long wavelength range; high photosensitivity at low light-intensity levels and absorption by its intermediates over the entire visible range[35]. Upon absorption of blue light at 447 nm, molecules of the initial D-state get excited to the L-state with maximum absorption wavelength at 660 nm. The L-state exhibits reverse saturable absorption (RSA) over a wide range, i.e. 500–700 nm, where the absorption cross-section of the L-state is greater than that of the D- and S-states, which do not show any absorption. The quantum efficiency of the L-state formation is 0.88, out of which 50% of L-state decays to the adduct S-state and the rest returns back to the initial ground D-state. These intermediates are photochemically switched back to the initial state by shinning light at a wavelength corresponding to the absorption peak of that intermediate[35,39]. These unique properties can be extremely useful for a variety of applications based on nonlinear absorption.

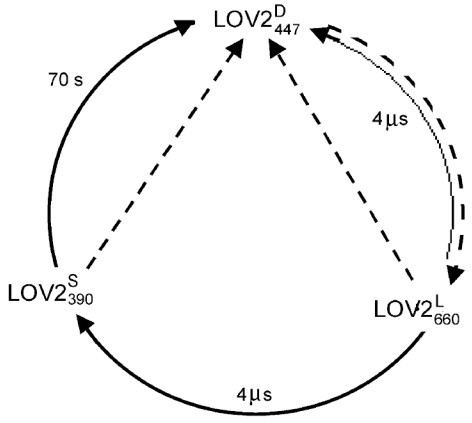

Figure 1. Schematic of the photochemical cycle of LOV2. Subscripts indicate absorption peaks (in nm). Solid and dashed arrows represent thermal and photoinduced transitions, respectively.

The spectral and kinetic properties of LOV2 domain can be altered by changing the pH value and addition or substitution of chemical groups, etc.[35,39]. For instance, in the LOV2-C39A mutant, substitution of cysteine[39] with alanine precludes the formation of the S-state and therefore, the L-state of this mutant decays back to the ground state[35] with a time constant of 72 μs. Substitution of additional amino acids results in various mutants of LOV2 that include[36] S20F, F23Y, N38D, R40D and Q43H.

We have recently reported a detailed theoretical analysis of all-optical switching in LOV2 phototropin based on excited-state absorption, using pulsed pump beams and have shown the applicability of the switching characteristics to the design of all-optical NOT, NOR and NAND logic gates[40]. In this communication, we theoretically analyse all-optical light modulation of a cw probe laser beam at 660 nm corresponding to the peak absorption of the L-state, by cw and pulsed pump laser beams at 442 nm, corresponding to the peak absorption wavelength of the initial D-state in LOV2 domain from *A. sativa* (oat) Phot1. The switching characteristics are based on nonlinear excited-state absorption and have been analysed using the rate equation approach. The effect of various parameters such as small-signal absorption coefficient (β), rate constants of the L-state and absorption cross-section of the ground state on modulation has been analysed in detail. The modulation characteristics have also been used to estimate properties of optically-addressed SLMs or input–output transducers that are basic elements in real-time optical signal processing and computing systems. They find wide applications as input and output transducers for image amplification, time/space transformation, scratch-pad memory, programmable detector masking and page composition for holographic and three-dimensional memories. Combined with Fourier transform, SLMs are capable of performing useful processing operations, including image addition and subtraction, logic operations, edge enhancement and thresholding[9,10,15,41,42].

We first consider wild-type (WT) LOV2 molecules exposed to a light beam of intensity I'_m, which modulates the population densities of different states through the excitation and de-excitation processes that can be described by the rate equations in the following form[9–13],

$$\frac{dN_D}{dt} = -\psi_{DL}\sigma_D I_m N_D + (\psi_{LD}k_{LD} + I_m\sigma_L)N_L + (k_{SD} + I_m\sigma_S)N_S, \quad (1)$$

$$\frac{dN_L}{dt} = \psi_{DL}\sigma_D I_m N_D - (\psi_{LD}k_{LD} + \psi_{LS}k_{LS} + I_m\sigma_L)N_L, \quad (2)$$

$$\frac{dN_S}{dt} = \psi_{LS} k_{LS} N_L - (k_{SD} + I_m \sigma_S) N_S, \quad (3)$$

where σ_i, i = D, L and S are absorption cross-sections of the three states; I_m is the photon density flux of the modulation laser beam, i.e. ratio of the intensity I'_m to the photon energy $h\nu$. $\psi_{DL} = 0.88$ is the quantum efficiency for the formation of the L-state and $\psi_{LD} = \psi_{LS} = 0.5$ are the transition probabilities for the transitions L → D and L → S, respectively[35]. The rate constants k_{LD}, k_{LS} and k_{SD} represent transitions from L → D, L → S and S → D respectively.

The light-induced population densities in the various levels at steady state are given by

$$N_i = N_D I_m P^{-1} \begin{pmatrix} I_m^{-1} P \\ \psi_{DL} \sigma_D \\ \psi_{DL} \psi_{LS} k_{LS} \sigma_D Q^{-1} \end{pmatrix}, \quad (4)$$

where $N_D = N/X$ is the population density in the D-state, $P = \psi_{LD} k_{LD} + \psi_{LS} k_{LS} + I_m \sigma_L$, $Q = k_{SD} + I_m \sigma_S$,

$$X = \left[1 + \frac{\psi_{DL} I_m \sigma_D}{P} \left(1 + \frac{\psi_{LS} k_{LS}}{Q} \right) \right]$$

and $N = N_D + N_L + N_S$ is the total number of active LOV2 molecules.

We consider the transmission of a weak cw probe laser beam of intensity I'_p ($I'_p \ll I'_m$) at 660 nm corresponding to the peak absorption of the L-intermediate in the LOV2 photocycle, modulated by absorption due to excitation of the molecules by the cw laser beam at 442 nm. As $\sigma_{Dp} = \sigma_{Sp} = 0$ at the probe wavelength, the absorption coefficient of the probe beam can be written as

$$\alpha_p(I_m) = N_L(I_m) \sigma_{Lp}, \quad (5)$$

where subscript p denotes the value at probe wavelength. Propagation of the probe beam through the LOV2 sample is governed by,

$$\frac{dI'_p}{dx} = -\alpha_p(I_m) I'_p, \quad (6)$$

where x is the distance in the medium.

The modulation characteristics can be computed by integrating eq. (6). The result in the form of normalized transmitted probe intensity (NTPI) is given by

$$\frac{I_{pout}}{I_{pin}} = \exp\left(-\frac{\beta}{X} \frac{\psi_{DL} I_m \sigma_D}{P} \right), \quad (7)$$

where the small-signal absorption coefficient $\beta = N \sigma_{Lp} L$.

The transmission characteristics, namely variation of NTPI at 660 nm with I'_m at 442 nm have been simulated using eqs (1)–(7), for LOV2-WT phototropin with typical values of absorption cross-section and rate constants reported in the literature[35], i.e. $\sigma_D = 5.0 \times 10^{-17}$ cm^2, $\sigma_L = 1.5 \times 10^{-17}$ cm^2, $\sigma_S = 5.8 \times 10^{-18}$ cm^2, $\sigma_{Lp} = 2.1 \times 10^{-17}$ cm^2, $k_{LS} = k_{LD} = 2.5 \times 10^5$ s^{-1}, $k_{SD} = 1.42 \times 10^{-2}$ s^{-1} and with sample thickness L = 2 mm.

The transmission characteristics of LOV2-WT and its mutant LOV2-C39A for different values of β are shown in Figure 2, with solid and dashed lines respectively. Increase in I'_m leads to increase in the population of the L-state and hence increased absorption of the probe beam. It is evident that NTPI decreases considerably with increase in I'_m and saturates at higher pump intensities. The percentage modulation is larger in LOV2-C39A than in LOV2-WT at comparatively lower values of I'_m (~1 kW/cm^2) and transmission of the probe beam saturates at lower values of I'_m in LOV2-C39A. Percentage modulation of the probe beam intensity in LOV2-WT for β = 0.2 and 5 at I'_m = 50 kW/cm^2 is 11.85 and 95.73, respectively. For LOV2-C39A, the percentage modulation for the same values of β at I'_m = 1 kW/cm^2 is 12.63 and 96.58 respectively. The probe beam gets completely switched, i.e. 100% modulated in LOV2-WT and in LOV2-C39A at I'_m = 50 kW/cm^2 and 1 kW/cm^2 respectively, for β = 8. This is due to the fact that the absorption cross-section of the ground state at probe wavelength $\sigma_{Dp} = 0$.

Figure 3 shows variation in the normalized population density of the different intermediates of LOV2-WT with I'_m. Initially, at lower values of I'_m, the population of the S-state increases rapidly due to the shorter lifetime of the L-state. This can be seen in the magnified view in Figure 3 (inset). The population of the L-state is thus negligible. After a certain value of I'_m, the population of the S-state decreases due to absorption of the modulation beam by

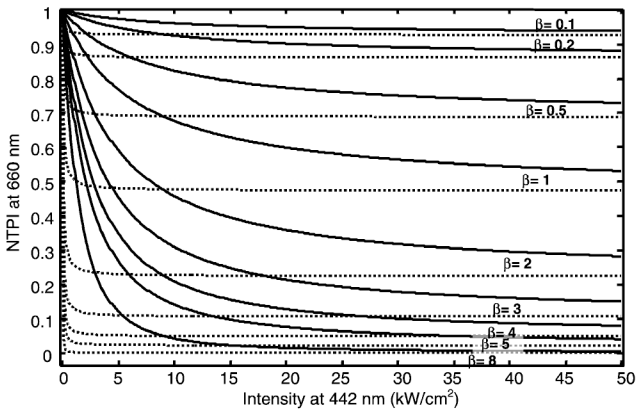

Figure 2. Variation of NTPI at 660 nm with I'_m for LOV2-WT (solid lines) and LOV2-C39A mutant (dashed lines) respectively, for different values of β, with $\sigma_{Lp} = 2.1 \times 10^{-17}$ cm^2.

the S-state itself, resulting in an increase in the population of the L-state. There is a slight increase in the population of the initial D-state also, as shown in Figure 3.

The effect of the rate constant k_{LD} on NTPI is shown in Figure 4. As k_{LD} decreases the percentage modulation increases, as an increase in the lifetime of the L-state increases the population of the L-state, which leads to increased absorption of the probe beam. Variation in k_{LS} leads to a similar effect with the transmission saturating at lower pump intensities for lower values of k_{LS}, as shown in Figure 4 (inset). Figure 5 shows the effect of σ_D on NTPI. Higher values of σ_D also lead to higher population of the L-state and hence higher percentage modulation.

This switching mechanism in LOV2 can be utilized for the construction of a molecular SLM that will mainly depend on the optics of the pump and probe beams. Typical SLM properties can be estimated in the present case, for example, the dynamic range[10,16,17,41,42], $\delta = (I_{pout}/I_{pin})_{I'_m} / (I_{pout}/I_{pin})_{I'_m=0}$ and the sensitivity $S = -(\ln \delta)/I_m$. In LVO2 phototropin, the probe beam at 660 nm is only absorbed by the L-state as $\sigma_{Dp} = \sigma_{Sp} = 0$, which corresponds to the ideal case[10,16,17,41,42]. Hence, the variation of dynamic range with I'_m for this case will be same as that of NTPI as plotted in Figure 2. For LOV2-WT, $\delta = 0.53$ and $S = 1.26 \times 10^{-5}$ cm^2/W, at $I'_m = 50$ kW/cm^2, for $\beta = 1$, whereas for LOV2-C39A, $\delta = 0.51$ and $S = 6.73 \times 10^{-4}$ cm^2/W at $I'_m = 1$ kW/cm^2 for $\beta = 1$.

The switching characteristics can also be analysed by considering a Gaussian modulating pump pulse given by[12,40],

$$I'_m = I'_{m0} \exp\left(-c\left(\frac{t - t_m}{\Delta t}\right)^2\right), \quad (8)$$

where $c = 4\ln 2$ is the pulse profile parameter and Δt is the pulse width.

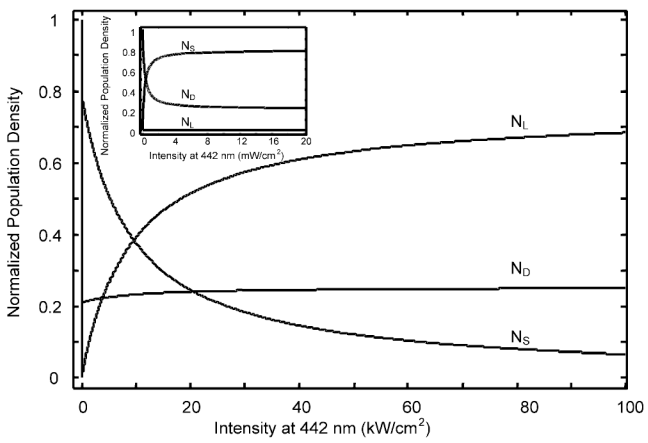

Figure 3. Variation of normalized population density with I'_m for different intermediate states of LOV2-WT. (Inset) Magnified variation at smaller values of I'_m.

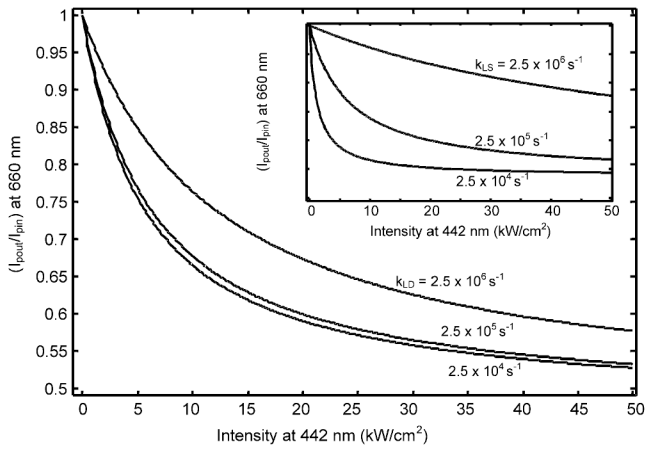

Figure 4. Variation of NTPI at 660 nm with I'_m for LOV2-WT for different values of rate constant k_{LD} with $\beta = 1$. (Inset) Corresponding variation for different values of rate constant k_{LS}, for $\beta = 1$.

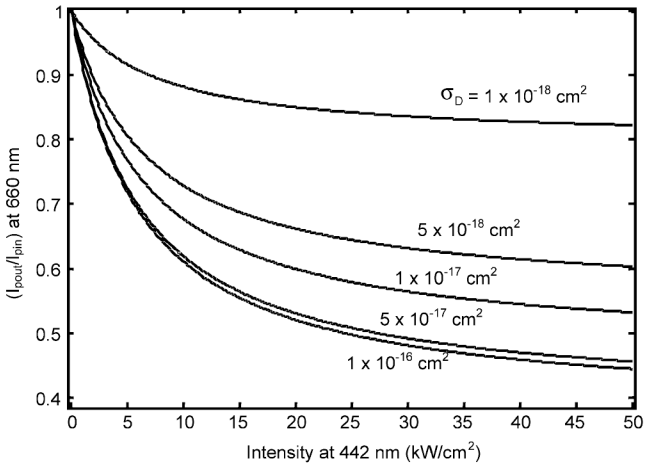

Figure 5. Variation of NTPI at 660 nm with I'_m for LOV2-WT for different values of σ_D, with $\beta = 1$.

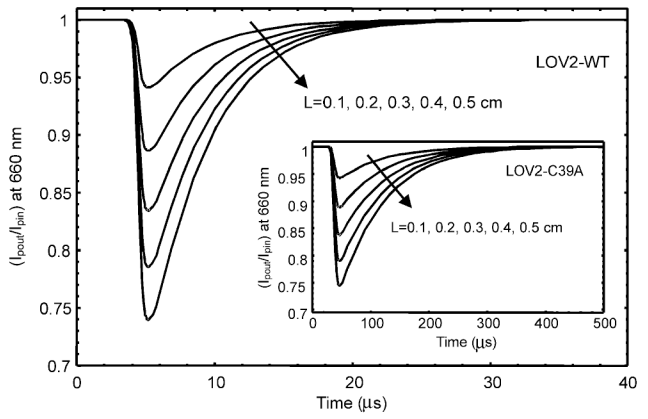

Figure 6. Variation of NTPI at 660 nm with time using a pulsed pump laser beam at 442 nm, for LOV2-WT for various values of sample thickness L, with $\Delta t = 1$ μs and $I'_{m0} = 50$ kW/cm^2. (Inset) Corresponding variation for LOV2-C39A with $\Delta t = 10$ μs and $I'_{m0} = 2$ kW/cm^2.

Variation in NTPI has been computed for LOV2-WT by numerically solving the rate equations for the intermediates with Δt = 1 μs and I'_m = 50 kW/cm^2. NTPI is initially high (switch-on state) due to no absorption, and becomes low (switch-off state), when a pulsed pump laser beam pumps the sample, enhancing the population of the L-state and increasing the absorption of the probe beam. Figure 6 shows the effect of sample thickness L on the transmission characteristics of LOV2-WT. The switching percentage increases with increase in L due to higher absorption. The switch-off and switch-on times for LOV2-WT are 1.6 μs and 22.3 μs respectively, for Δt = 1 μs, I'_m = 50 kW/cm^2, L = 2 mm and a concentration of 70 μM. The percentage modulation for L = 2 and 5 mm is 11.3 and 25.9%, respectively. The same percentage modulation can be achieved with LOV2-C39A mutant with Δt = 10 μs and at lower I'_m = 2 kW/cm^2, for the same path length and concentration as shown in Figure 6 (inset). The switch-off and switch-on times for LOV2-C39A are 21.2 μs and 0.42 ms respectively. Switching in LOV2-WT (~μs) based on excited-state absorption is much faster than in WT-bR, *p*pR or pR (~ms)[12,13,18,19].

In conclusion, we have conducted a detailed analysis of all-optical light modulation of a cw probe laser beam at 660 nm by a cw and a pulsed pump laser beam at 442 nm, using the recently discovered LOV2 phototropin blue-light plant photoreceptor. The present analysis highlights a number of advantages of LOV2 over other biomolecules such as bR, *p*pR and pR: (i) LOV2 has a simpler photocycle. (ii) It has high quantum efficiency. (iii) There is no overlap in the absorption spectra of the initial state and the excited-state at probe wavelength (σ_{Dp} = 0), contrary to that observed in retinal proteins, hence 100% modulation can be achieved. (iv) The switching response is much faster in LOV2 (~μs) than in retinal proteins (~ms). (v) The switching response is faster in LOV2-WT than in the LOV2-C39A mutant, although it is at lower pump powers in the latter. (vi) Since the absorption spectra of LOV2 exhibit RSA over a wide range (500–700 nm), with almost constant absorption by the L-state[35], the modulation characteristics would be similar for probe beams at different wavelengths in this range, leading to broadband switching. (vii) As the properties of LOV2 can be tailored by physical, chemical and genetic engineering techniques, all-optical light modulation in LOV2 can be optimized for fast response, high-contrast and low-power operation. The present analysis shows the applicability of LOV2 phototropin as a new material for photonic applications.

1. Gubler, U. and Bosshard, C., A new twist in nonlinear optics. *Nature Mater.*, 2002, **1**, 209–210.
2. Skipetrov, S. E., Disorder is the new order. *Nature*, 2004, **432**, 285–286.
3. Guenther, B. D., Jopson, B., Koshel, R. J. and Paldus, B., Special Issue: Optics in 2005 Introduction. *Opt. Photon. News: Special Issue on Optics in 2005*, 2005, **16**, 14–44.
4. Kapteyn, H. C., Murnane, M. M. and Christor, I. P., Extreme nonlinear optics: Coherent X-rays from lasers. *Phys. Today*, 2005, **58**, 39–44.
5. Ravikanth, M. and Kumar, G. R., Nonlinear optical properties of porphyrins. *Curr. Sci.*, 1995, **68**, 1010–1017.
6. Stuart, J. A., Mercy, D. L., Wise, W. L. and Birge, R. R., Volumetric optical memory based on bacteriorhodopsin. *Synth. Met.*, 2002, **127**, 3–15.
7. Hampp, N., Bacteriorhodopsin as a photochromic retinal protein for optical memories. *Chem. Rev.*, 2000, **100**, 1755–1776.
8. Oesterhelt, D., Bräuchle, C. and Hampp, N., Bacteriorhodopsin: A biological material for information processing. *Q. Rev. Biophys.*, 1991, **24**, 425–478.
9. Roy, S., Singh, C. P. and Reddy, K. P. J., Generalized model for all-optical light modulation in bacteriorhodopsin. *J. Appl. Phys.*, 2001, **90**, 3679–3688.
10. Singh, C. P. and Roy, S., Analysis of low power spatial light modulation characteristics of bacteriorhodopsin. *Optik (Stuttgart)*, 2002, **113**, 373–381.
11. Roy, S., Singh, C. P. and Reddy, K. P. J., Analysis of all-optical switching in bacteriorhodopsin. *Curr. Sci.*, 2002, **83**, 623–637.
12. Singh, C. P. and Roy, S., All-optical switching in bacteriorhodopsin based on M state dynamics and its application to photonic logic gates. *Opt. Commun.*, 2003, **218**, 55–66.
13. Roy, S., Sharma, P., Dharmadhikari, A. K. and Mathur, D., All-optical switching with bacteriorhodopsin. *Opt. Commun.*, 2004, **237**, 251–256.
14. Sharma, P. and Roy, S., All-optical spatial light modulation in pharaonis phoborhodopsin and its application to parallel logic gates. *J. Appl. Phys.*, 2004, **96**, 1687–1695.
15. Sharma, P. and Roy, S., All-optical biomolecular logic gates with bacteriorhodopsin. *IEEE Trans. Nanobiosci.*, 2004, **3**, 129–136.
16. Singh, C. P., Sharma, P. and Roy, S., Spatial light modulation with *pharaonis* phoborhodopsin. *IEE Proc. Cir. Dev. Syst.*, 2003, **150**, 563–568.
17. Sharma, P., Roy, S. and Singh, C. P., Low power spatial light modulator with pharaonis phoborhodopsin. *Thin Solid Films*, 2005, **477**, 227–232.
18. Roy, S., Kikukawa, T., Sharma, P. and Kamo, N., All-optical switching in *pharaonis* phoborhodopsin protein molecules. *IEEE Trans. Nanobiosci.*, 2006, **5**, 178–187.
19. Roy, S. and Sharma, P., Analysis of all-optical light modulation in proteorhodopsin protein molecules. *Optik* (in press).
20. Béjà, O. *et al.*, Bacterial rhodopsin: Evidence for a new type of phototrophy in the sea. *Science*, 2000, **289**, 1902–1906.
21. Béjà, O., Spudich, E. N., Spudich, J. L., Leclerc, M. and DeLong, E. F., Proteorhodopsin phototrophy in the ocean. *Nature*, 2001, **411**, 786–789.
22. Dioumaev, A. V., Brown, L. S., Shih, J., Spudich, E. N., Spudich, J. L. and Lanyi, J. K., Proton transfers in the photochemical reaction cycle of proteorhodopsin. *Biochemistry*, 2002, **41**, 5348–5358.
23. Friedrich, T. *et al.*, Proteorhodopsin is a light-driven proton pump with variable vectoriality. *J. Mol. Biol.*, 2002, **321**, 821–838.
24. Váró, G., Brown, L. S., Lakatos, M. and Lanyi, J. K., Photocycle of halorhodopsin from *Halobacterium salinarium*. *Biophys. J.*, 2003, **84**, 1202–1207.
25. Briggs, W. R. *et al.*, The phototropin family of photoreceptors. *Plant Cell*, 2001, **13**, 993–997.
26. Hegemann, P., Fuhrmann, M. and Kateriya, S., Algal sensory photoreceptors. *J. Phycol.*, 2001, **37**, 668–676.
27. Briggs, W. R. and Christie, J. M., Phototropins 1 and 2: Versatile plant blue light receptors. *Trends Plant Sci.*, 2002, **7**, 204–210.
28. Penzkofer, A., Endres, L., Schiereis, T. and Hegemann, P., Yield of photo-adduct formation of LOV domains from *Chlamydomonas reinhardtii* by picosecond laser excitation. *Chem. Phys.*, 2005, **316**, 185–194.

29. Holzer, W., Penzkofer, A. and Hegemann, P., Photophysical and photochemical excitation and relaxation dynamics of LOV domains of phot from *Chlamydomonas reinhardtii*. *J. Lumin.*, 2005, **112**, 444–448.
30. Holzer, W., Penzkofer, A. and Hegemann, P., Absorption and emission spectroscopic characterisation of the LOV2-His domain of phot from *Chlamydomonas reinhardtii*. *Chem. Phys.*, 2005, **308**, 79–91.
31. Salomon, M. *et al.*, An optomechanical transducer in the blue light receptor phototropin from *Avena sativa*. *Proc. Natl. Acad. Sci. USA*, 2001, **98**, 12357–12361.
32. Harper, S. M., Neil, L. C. and Gardener, K. H., Structural basis of a phototropin light switch. *Science*, 2003, **301**, 1541–1544.
33. Schuttrigkeit, T. A., Kompa, C. K., Salomon, M., Rudiger, W. and Michel-Beyerle, M. E., Primary photophysics of the plant blue light receptor phototropin of *Avena sativa*. *Chem. Phys.*, 2003, **294**, 501–508.
34. Kennis, J. T. M., Crosson, S., Gauden, M., Stokkum, I. H. M. V., Moffat, K. and Grondelle, R. V., Primary reaction of the LOV2 domain of the phototropin, a plant blue light photoreceptor. *Biochemistry*, 2003, **42**, 3385–3392.
35. Swartz, T. E., Corchnoy, S. B., Christie, J. M., Lewis, J., Szundi, I., Briggs, W. R. and Bogomolni, R., The photocycle of a flavin binding domain of the blue light photoreceptor phototropin. *J. Biol. Chem.*, 2001, **276**, 36493–36500.
36. Salomon, M., Christie, J. M., Knieb, E., Lempert, U. and Briggs, W. R., Photochemical and mutational analysis of the FMN-binding domains of the plant blue light receptor, phototropin. *Biochemistry*, 2000, **39**, 9401–9410.
37. Corchnoy, S. B., Swartz, T. E., Lewis, J. W., Szundi, I., Briggs, W. R. and Bogomolni, R. A., Intramolecular proton transfers and structural changes during the photocycle of the LOV2 domain of phototropin 1. *J. Biol. Chem.*, 2003, **278**, 724–731.
38. Kennis, J. T. M., Stokkum, I. H. M. V., Crosson, S., Gauden, M., Moffat, K. and Grondelle, R. V., The LOV2 domain of phototropin: A reversible photochromic switch. *J. Am. Chem. Soc.*, 2004, **126**, 4512–4513.
39. Guo, H., Kottke, T., Hegemann, P. and Dick, B., The phot LOV2 domain and its interaction with LOV1. *Biophys. J.*, 2005, **89**, 402–412.
40. Roy, S. and Kulshrestha, K., All-optical switching in plant blue light photoreceptor phototropin. *IEEE Trans. Nanobiosci.*, 2006, **5**, 281–287.
41. Roy, S., Singh, C. P. and Reddy, K. P. J., Analysis of spatial light modulation characteristics of C_{60}. *Appl. Phys. Lett.*, 2000, **77**, 2656–2658.
42. Roy, S. and Kulshrestha, K., Theoretical analysis of all-optical spatial light modulation in organometallics based on triplet state absorption dynamics. *Opt. Commun.*, 2005, **252**, 275–285.

ACKNOWLEDGEMENTS. We thank the Department of Science and Technology, New Delhi for partial support. We also thank Prof. A. Penzkofer, University of Regensburg, Germany for helpful discussions.

Received 15 February 2006; revised accepted 29 November 2006

Insecticide resistance in malaria vector *Anopheles culicifacies* in some tribal districts of Chhattisgarh, India

S. N. Sharma[1], R. P. Shukla[1], P. K. Mittal[2], T. Adak[2,*] and Sarala K. Subbarao[3]

[1]Malaria Research Centre, Field Station, Inderjeet Garden, Bhotia Parao, Haldwani, Nainital 263 141, India
[2]Malaria Research Centre (ICMR), 2, Nanak Enclave, Delhi 110 009, India
[3]Malaria Research Centre (ICMR), Sham Nath Marg, Delhi 110 054, India

Insecticide resistance in *Anopheles culicifacies*, the major vector of malaria in tribal areas of Chhattisgarh, was determined using standard WHO susceptibility tests. Majority of the districts in Chhattisgarh are highly malaria-prone and under the Enhanced Malaria Control Project (EMCP), where synthetic pyrethroids are used for indoor spraying against *An. culicifacies*. Resistance/susceptibility of *An. culicifacies* to DDT (4%), malathion (5%) and deltamethrin (0.05%) was studied in a few villages of Kanker and Jagdalpur, Mahasamund and Raigarh Districts. The corrected mortality varied from 13.8 to 25% to DDT, 59.3 to 87.9% to malathion and 89.4 to 92.5% to deltamethrin. The tests also revealed a higher knock-down time for *An. culicifacies* collected from the Kanker and Jagdalpur Districts where synthetic pyrethroid is being sprayed, indicating incipient resistance to synthetic pyrethroid in this vector species.

Keywords: *Anopheles culicifacies*, insecticides, malaria vector, resistance.

ANOPHELES CULICIFACIES is the major malaria vector of rural and peri-urban plain areas in India and contributes to the transmission of about 65% of the total malaria cases[1]. The main target of the National Vector Borne Disease Control Programme (NVBDCP), formerly known as National Anti Malaria Programme (NAMP) of India, is to control malaria transmitted by *An. culicifacies* in rural areas by Indoor Residual Spraying (IRS) of insecticides. At present, DDT (organochlorine), malathion (organophosphorus), and deltamethrin, lamdacyhalothrin, cyfluthrin, etc. (synthetic pyrethroids) are the commonly used insecticides in India for IRS. However, due to the constant use of DDT during the past five decades, resistance in *An. culicifacies* is now widespread throughout the country[2–4], except in some areas where DDT is still in use, as it is still an effective tool to control *An. fluviatilis*-transmitted *Plasmodium falciparum*-malaria[5]. During the sixties, HCH (another organochlorine insecticide) was also used for IRS in areas where DDT resistance was detected. How-

*For correspondence. (e-mail: adak.mrc@gmail.com)